

## Article

# Fire Performance of Intumescent Waterborne Coatings with Encapsulated APP for Wood Constructions

Atif Hussain <sup>1</sup>, Véronic Landry <sup>1</sup>, Pierre Blanchet <sup>1,\*</sup>, Doan-Trang Hoang <sup>1</sup> and Christian Dagenais <sup>1,2</sup>

<sup>1</sup> NSERC Industrial Research Chair on Ecoresponsible Wood Construction, Department of Wood and Forest Sciences, Université Laval, Quebec, QC G1V 0A6, Canada; A.Hussain@bath.edu (A.H.); veronic.landry@sbf.ulaval.ca (V.L.); thi-doan-trang.hoang.1@ulaval.ca (D.-T.H.); christian.dagenais@fpinnovations.ca (C.D.)

<sup>2</sup> FPInnovations, 1055 rue du PEPS, Quebec, QC G1V 4C7, Canada

\* Correspondence: pierre.blanchet@sbf.ulaval.ca

**Abstract:** In this work, intumescent coatings were prepared for protection of wood from fire. The fire-retardant chemical ammonium polyphosphate (APP) is known to have poor resistance to water and high humidity as it is hygroscopic in nature. To improve the water resistance, durability and fire resistance of the intumescent coating, APP was modified using a hybrid organic-inorganic polysiloxane encapsulation shell prepared by the sol-gel method. The physical and chemical properties of the intumescent mix containing microencapsulated ammonium polyphosphate (EAPP) particles were characterized by X-ray fluorescence (XRF), Fourier transform infrared spectroscopy (FTIR), water absorption, dynamic vapor sorption (DVS) and thermogravimetric analysis (TGA). The EAPP mix showed 50% reduction in water absorption, 75% reduction in water vapor sorption and increased thermal stability when compared to the APP mix. The intumescent coatings were applied on wood samples, and their fire performance was evaluated using a cone calorimeter test. The intumescent coatings containing EAPP mix showed better fire retarding properties with longer time to ignition, lower heat release rate and shorter heat release peak when compared to the coating without EAPP mix. The prepared intumescent coating shows higher resistance to water and moisture, and it has great potential to be used in bio-based construction industry for enhancing the fire resistance of wood.

**Keywords:** intumescent; coating; microencapsulation; fire resistance; cone calorimeter



**Citation:** Hussain, A.; Landry, V.; Blanchet, P.; Hoang, D.-T.; Dagenais, C. Fire Performance of Intumescent Waterborne Coatings with Encapsulated APP for Wood Constructions. *Coatings* **2021**, *11*, 1272. <https://doi.org/10.3390/coatings11111272>

Academic Editor: Michael A. Delichatsios

Received: 29 September 2021  
Accepted: 18 October 2021  
Published: 20 October 2021

**Publisher's Note:** MDPI stays neutral with regard to jurisdictional claims in published maps and institutional affiliations.



**Copyright:** © 2021 by the authors. Licensee MDPI, Basel, Switzerland. This article is an open access article distributed under the terms and conditions of the Creative Commons Attribution (CC BY) license (<https://creativecommons.org/licenses/by/4.0/>).

## 1. Introduction

Wood is an outstanding material that has been widely used in construction due to its unique properties such as low density, good mechanical and physical properties, environmental friendliness and natural beauty. Some of the major concerns regarding the use of wood products are its durability and flammability [1,2]. Treatments with flame retardant additives have been used for improving the fire resistance properties of wood and delaying fire propagation through building structures [3,4]. In terms of treatment application, coatings are generally preferred over wood impregnation as they are economical, less time consuming and do not cause swelling or shrinkage of the substrate [5]. Moreover, coatings provide an insulation barrier isolating the substrate from heat flux and influencing its ignition, thermal degradation and combustion characteristics [6].

More recently, intumescent fire retardant coatings have been used for protection of wood and steel in buildings, chemical plants and other facilities [7–9]. Intumescent coatings are composed of three main fire retardant additives: (i) an acid source (such as ammonium polyphosphate, APP), which is usually a carbonized accelerator or a dehydrating agent generating acid compounds in situ; (ii) a blowing agent (such as melamine, MEL), which is an important ingredient for production of gases when heated; and (iii) a carbon source (pentaerythritol, PER), which is the char forming agent insulating the underlying substrate and maintaining structural integrity [10–13]. The three components of the intumescent

coating are bound together using a polymeric binder (such as polyvinyl acetate-ethylene). Intumescent coatings have advantages over non-intumescent coatings being more efficient for protecting wood from fire [14]. Furthermore, intumescent coatings expand when heated beyond their critical temperature forming a charred multilayer [11].

However, there are concerns related to fire retardant coatings especially when used outdoors. The coatings tend to lose their performance as fire retardant chemicals can leach from the wood surface in presence of rain or even high humidity levels leaving the substrate unprotected from fire. Fire retardant additives in intumescent coatings such as APP are hygroscopic in nature, and when exposed to high humidity or rain, they tend to hydrolyze water-soluble components [6,15]. As a result, intumescent coatings have limited usage in exterior wood sidings as well as in indoor spaces with high relative humidity levels. Furthermore, typical intumescent coatings are opaque which can compromise the natural appearance of wood. To address these issues, some of the techniques developed for protection of fire retardants include surface modification with coupling agents, ultra-fine modification and microencapsulation [8,16–20].

Microencapsulation has been reported to be an effective strategy to modify the flame retardant while playing a synergistic role in flame retardancy [21–23]. Many studies have reported the use of silane coupling agents, bio-based macromolecules, ionic liquids and melamine-based resins for the modification of flame retardant additives and achieved good results [24–27].

In previous work, polysiloxane microencapsulation has shown to remarkably improve hydrophobicity of APP [28]. It was demonstrated earlier that the polysiloxane or silica microencapsulation of APP significantly improved flame retardancy of polyolefins [13,29]. Moreover, the combination of phosphorus and silicon based compounds has been shown to improve fire performance, and this synergistic effect is described as phosphorus promoting char formation and silicon forming a smooth layer protecting the formed char from oxidation [30]. In this study, an intumescent coating is prepared with microencapsulated APP, which was modified using an organic-inorganic hybrid polysiloxane shell. The intumescent coating containing microencapsulated APP is applied on wood and tested for its water resistance and flame retardancy. The effect of weathering on the performance of intumescent coatings applied on wood samples is also investigated.

## 2. Materials and Methods

The intumescent additives APP (InorFlam APP 201), MEL (InorFlam Melamine F40) and PER (InorFlam Penta M40) were provided by EMCO-Inortech Chemicals Inc. (Terrebonne, QC, Canada). The binder (vinyl acetate-ethylene copolymer Eco VAE401) was supplied by Celanese Ltd. (Dallas, TX, USA); prime pigment (TiO<sub>2</sub> Kronos 2310) and coalescent agent (Glycol ether PM acetate) were supplied by Univar Canada Ltd. (Montreal, QC, Canada). The solvent-free wetting and dispersing additive (BYK2010) and the VOC-free silicone-containing defoamer (BYK022) were provided by Dempsey (Montreal, QC, Canada).

The microencapsulated APP (EAPP) used in this study were prepared in accordance with previous work [28]. Ethanol (150 mL) and water (50 mL) were stirred at 700 rpm for 10 min using a magnetic stirrer. APP (50 g) was added and stirred at 1000 rpm for 15 min. Ammonia water (17 mL) was added and stirred for 20 min. Tetraethoxysilane (10 mL) was added dropwise and stirred for 10 min. Finally, methytriethoxysilane (2.5 mL) was added and stirred at for 4 h at 1000 rpm. The final mixture was filtered and washed with water and dried at 80 °C until constant mass was reached. All of the raw materials were used without any further purification. The chemical composition and typical characteristics of the raw materials are detailed in Table 1.

**Table 1.** Main characteristics of raw materials used in this study to prepare the formulation.

Component	Chemical Composition	Average Particle Size ( $\mu\text{m}$ )	Content Wt.% Solids (%)
Ammonium polyphosphate (APP)	( $\text{NH}_4\text{PO}_3$ ) <sub>n</sub> (n > 1000) crystalline form II 31% w/w P content 14% w/w N content	$\leq 15 \mu\text{m}$	100
Melamine (MEL)	1,3,5-Triazine-2,4,6-triamine	$\leq 40 \mu\text{m}$	100
Pentaerythritol (PER)	2,2-Bis(hydroxymethyl)1,3-propanediol	$\leq 40 \mu\text{m}$	$\geq 98$
Binder ECO VAE401	vinyl acetate-ethylene copolymer		54–58
Prime pigment KRNO52310	Titanium dioxide	$\geq 0.1$	95–100% $\text{TiO}_2$ 1–5% $\text{Al}(\text{OH})_3$
Coalescent agent	2-methoxy-1-methylethyl acetate	-	>99
Wetting and Dispersing agent BYK2010	Aqueous emulsion of a structured acrylate copolymer with pigment-affinic groups.	-	-
Defoaming agent BYK022	Mixture of foam-destroying polysiloxanes and hydrophobic solids in polyglycol	-	-
Microencapsulated APP (EAPP)	APP encapsulated by polysiloxane	$10 \pm 2$	-

## 2.1. Materials

### 2.1.1. Preparation of Intumescent Powder Blend

Two intumescent blends (Table 2) were prepared for this study: (i) APP mix (control mixture) containing APP, MEL and PER and (ii) EAPP mix containing EAPP, MEL and PER. The blends were vigorously agitated for 15 min using a mechanical stirrer at room temperature.

**Table 2.** List of intumescent blends and coatings used in this study.

Sample	Description
APP Mix	APP, MEL and PER
EAPP Mix	Microencapsulated APP, MEL and PER
APP Coating	APP mix + dispersing agent, pigment, defoaming agent, binder, coalescent agent and water
EAPP Coating	EAPP mix + dispersing agent, pigment, defoaming agent, binder, coalescent agent and water
APP Coated Wood	Wood samples coated with APP Coating
EAPP Coated Wood	Wood samples coated with EAPP Coating
Aged APP Coated Wood	Wood samples coated with APP Coating after weathering
Aged EAPP Coated Wood	Wood samples coated with EAPP Coating after weathering

The APP mix was prepared by mixing the components APP: MEL: PER in the ratio 3:1:1, respectively. The EAPP mix was prepared by substituting the APP with MAPP, although the quantity of APP was kept constant in both intumescent mixtures for comparing the properties between the two intumescent blends. Therefore, to prepare the EAPP mix with the equivalent weight of APP in the APP mix, the quantity of APP present in EAPP was calculated by X-ray fluorescence (XRF) analysis.

From the data shown in Table 3, it was found that for each molecule of EAPP, the weight percentage of silicon was twice that of phosphorus. This means that the weight of the polysiloxane encapsulation is roughly twice the weight of APP. From the calculations using the data in Table 3, it was determined that the weight of EAPP that had to be added

to the EAPP mix was thrice the weight of APP particles added to the APP mix. Hence, the EAPP mix contained the components EAPP:MEL:PER in the ratio 9:1:1.

**Table 3.** Elemental composition of the EAPP particles.

Test Sample	Elemental Composition (%)			Si/P
	Si	O	P	
1	20.63	68.48	10.89	1.90
2	21.21	68.40	10.39	2.04
3	21.09	68.42	10.50	2.01
4	21.32	68.38	10.30	2.07

### 2.1.2. Preparation of Intumescent Waterborne Coating

Two intumescent waterborne coating formulations were prepared using the APP mix and EAPP mix using the process described in Table 4. The APP Coating formulation contained the APP mix, dispersing agent, pigment, defoaming agent, binder, coalescent agent and water. The other EAPP coating formulation contained all the above ingredients except APP mix which was replaced by EAPP mix. A scheme diagram showing the deposition of APP and EAPP coating is presented in Figure 1. The optimal mass ratio of the components was determined through a series of formulation tests. This selected weight ratio allowed the best solids dispersion. The coating formulations were obtained as a dispersion using a high-speed disperser (Dissolver Dispermat LC 30, VMA-Getzmann GmbH, Reichshof, Germany) and speeds ranging from 800 to 2500 rpm.

Due to the high solid content of the intumescent coatings and the difficult dispersion of the EAPP particles, multiple smaller batches (100 g each) were prepared to ensure maximum dispersion of the solid particles. Special attention was taken to avoid overheating of the mixture, since this may cause premature degradation. The prepared intumescent coatings had a high solid concentration with 60.08% for APP Coating and 69.13% for EAPP Coating.

**Table 4.** Basic formulation for the intumescent waterborne coatings.

Steps	Ingredients	Batch (wt.%)	
		APP Coating	EAPP Coating
Step 1 (10 min, 800 rpm)	Water	20.00	40.91
	Dispersing agent (Byk-2010)	1.21	1.83
Step 2 (30 min, 2500 rpm)	TiO <sub>2</sub> Pigment	4.00	6.06
	Intumescent Blend	44.16	15.39
	Water	7.00	-
	Defoaming agent (Byk-022)	0.88	1.34
Step 3 (20 min, 1700 rpm)	Binder	20.75	31.44
	Coalescent agent	2.00	3.03
-	Total	100.00	100.00

### 2.1.3. Preparation of Water Based Epoxy Primer

A dual component water-based epoxy primer was used to improve the adherence between wood substrate and the intumescent coating. The primer formulation and ingredients were provided by EMCO-Inortech Chemicals Inc. (Terrebonne, QC, Canada) and used as received. The system was prepared by mixing the supplied epoxy resin and curing agent binder with a volume ratio of 3:1, respectively, for 10 min at 1000 rpm. The mixture was then left for 30 min before its application on the wood substrate.

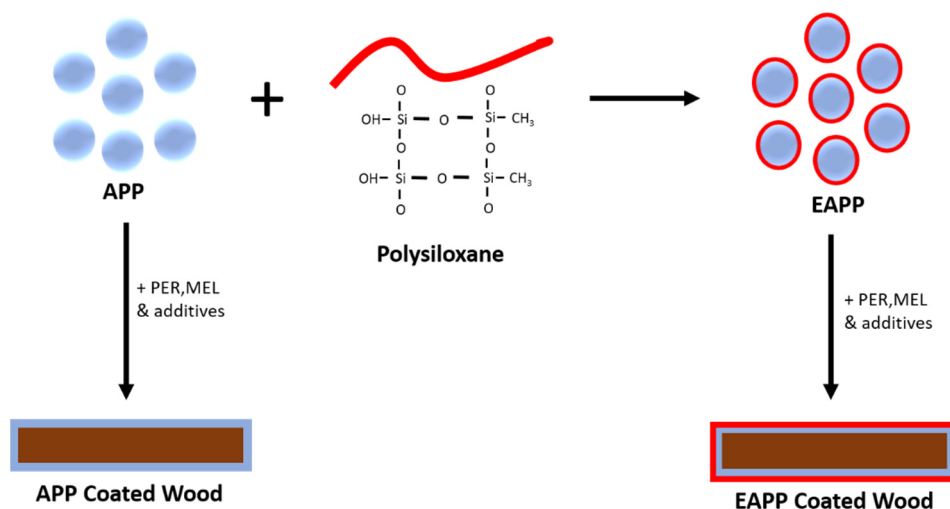


**Figure 1.** Scheme showing APP encapsulation and coating on wood substrate.

#### 2.1.4. Wood Sample Preparation

White spruce (*Picea glauca* (Moench) Voss) wood panels (100 mm × 100 mm × 16 mm) were prepared. The samples were conditioned in a climate-controlled room at 20 °C and 50% relative humidity (RH) until they reached constant mass. The wooden panels were disc-sanded on the flat grain using P150 grit paper.

#### 2.1.5. Coating Deposition

The formulated coatings were applied on the wood samples with an automatic film applicator equipped with a bar coater (BYK-Gardner, Columbia, DC, USA) at a constant speed of 50 mm/s. For the wood samples, three layers of coatings were applied including one coat of primer (approx. 200 µm wet thickness) and two layers of intumescent coatings (approx. 75 µm each of wet film thickness). The thickness of the dry coating was evaluated with a digital microscope. Two layers of 150 µm each of wet coating were applied on glass panels. The samples were then left to stabilize at room temperature for at least one week before conducting the analysis.

### 2.2. Methods

#### 2.2.1. X-ray Fluorescence (XRF) Analysis

The XRF spectrometry was performed for quantitative determination of the atomic ratio of phosphorus and silicon, which are the important characteristic elements of APP and polysiloxane, respectively, in EAPP specimen. The analysis was carried out under mechanical vacuum in a micro-XRF analyzer (M4 Tornado model from Bruker, Billerica, MA, USA) equipped with a rhodium X-ray tube and two EDS detectors. The homogenous powder specimen was placed between two SPEX 3525 Ultralene film (4 µm thickness). Four analyses were conducted, and the average value was reported.

#### 2.2.2. Dynamic Vapor Sorption Isotherm and Water Uptake

A vapor sorption apparatus, the VTI-SA+ Analyzer (TA Instruments, New Castle, DE, USA), was used to calculate the sorption isotherms of the intumescent blends and the water uptake of the coating films. Approximately 10–15 mg of sample was placed in a pan, combined with a microbalance by a hanging wire. The sample was then exposed to varying relative humidity (RH) levels, increasing in steps from 0 to 95% and then decreasing the RH back to 0% in the same manner. Each RH step was programmed to move to the next step when the change in sample mass was stable for at least 10 min ( $dm/dt < 0.002\%$ ), which would allow to obtain equilibrium moisture content values as reported earlier. The maximum time allowed for each RH step was 180 min, and the data were recorded every

10 s during the experimental run. For the water uptake experiment, the samples were exposed to maximum RH level for 300 min. The temperature was maintained at 23 °C throughout the experiments. The test was performed in triplicates.

#### 2.2.3. Thermogravimetric and Differential Thermogravimetric Analysis (TG/DTG)

Thermogravimetric analysis was performed for the samples from 25 to 800 °C at a heating rate of 10 °C·min<sup>-1</sup> in air atmosphere in a thermogravimetric analyzer. The coating formulations were deposited on glass, allowed to dry and were then detached from the glass substrate for analysis. The weight of all samples was kept at approximately 5 mg, and three measurements were taken for each formulation.

#### 2.2.4. Fourier Transform-Infrared (FTIR) Spectroscopy

The presence of characteristic absorption bands was studied by ATR-FTIR spectroscopy (Model Spectrum 400 model, Perkin Elmer, Waltham, MA, USA) using a crystal diamond accessory. Absorption spectra were recorded for a wavelength range from 4000 to 650 cm<sup>-1</sup>. A total of 32 scans were taken, and the resolution was set to 4 cm<sup>-1</sup>. Three analyses were performed for each sample.

#### 2.2.5. Accelerated Aging Tests

In order to compare the water-resistance between APP Coating and EAPP Coating on wood, the samples were exposed to artificial accelerated weathering test before further assessing their fire performance test. Tests were performed in a Ci3000+ Weather-Ometer (Atlas Materials Testing Solutions, Mount Prospect, IL, USA) following the ASTM G155-13 test method “Standard Practice for Operating Xenon Arc Light Apparatus for Exposure of non-metallic Materials”. This method allows the simulation of the weathering effects that occur when the materials are exposed to sunlight and moisture. The wood panels exposed consisted of 7 samples of each intumescent formulation. The samples underwent direct daylight exposure (Boro-Boro) at an Irradiance rate of 0.35 W/m<sup>2</sup>/nm and wavelength of 340 nm. The exposure cycle consisted of two steps. During the first step, the samples were exposed to light for 102 min at 50% RH and 63 ± 3 °C (black panel temperature). The second step consisted of exposure to light for 18 min under direct water spray. The exposure time for the accelerated aging test was 2000 h.

#### 2.2.6. Cone Calorimeter Test

An oxygen consumption cone calorimetry (Fire Testing Technology, West Sussex, UK) was used to carry out measurements on the samples according to the procedure defined in ISO 5660-1. All data were obtained at heat flux of 20, 35 and 50 kW/m<sup>2</sup>. The coated faces of specimens were exposed to the external heat source. A small spark igniter was placed above the specimen to allow pyrolysis gases to ignite. Before placing each sample horizontally in the metallic sample holder, the non-exposed area of sample was wrapped with aluminum foil. A lightweight mineral fiber blanket was used as an insulating between the non-exposed surface of sample and the metallic sample holder. The test was performed in triplicates for each sample, and the average reading was reported.

### 3. Results and Discussion

The water absorption curves of the two intumescent coatings are shown in Figure 2. The intumescent coating containing silica encapsulated APP (EAPP Coating) clearly shows a lower water absorption rate when compared to the intumescent coating containing non encapsulated APP (APP Coating). The water absorption curve of the EAPP Coating stabilizes after 2 h of exposure to 100% RH level. On the other hand, the APP Coating continues to absorb water throughout the experiment. At the end of test, the APP Coating curve shows a steady increase in water absorption predicting that the water saturation is significantly higher than that for the EAPP Coating.

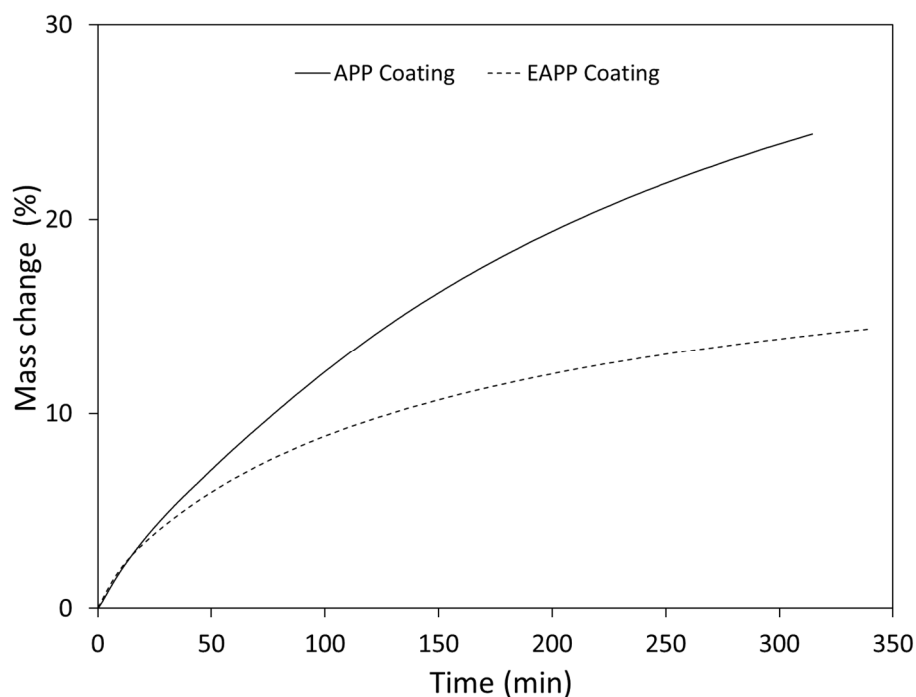


Figure 2. Water absorption curves of coating films.

The water vapor sorption isotherms of the intumescent powders are shown in Figure 3. Analyzing the adsorption curves of the mixes, the APP mix tends to adsorb slightly more water vapor on its surface when compared to microencapsulated powder containing EAPP. The mass change values of the intumescent powders increase with increasing relative humidity (RH). At 95% RH level, the mass change peak of the APP mix is prominent, showing that it is hygroscopic in nature compared to the EAPP particles in its mixture. It was reported earlier that APP microencapsulation could enhance its hydrophobicity and compatibility with polymers when used in coatings, thereby improving the dispersibility in the matrix [31,32].

The hysteresis between the adsorption and the desorption curve is more obvious for the APP mix meaning that the water molecules hold on to the surface of the APP [33]. In contrast, the EAPP mix shows almost negligible adsorption of water vapor on the surface at lower humidity levels. Moreover, the hysteresis between adsorption and desorption curves is hardly noticeable in the EAPP mix, meaning that microencapsulation has been able to protect the APP particles and eliminate their hygroscopic property responsible for their sensitivity to moisture [34].

The thermal stability of the intumescent blends was assessed by TGA. The decomposition of both samples took place in the range of 200–600 °C as seen in Figure 4. The DTG curves presented in Figure 5 show multiple small peaks and a large peak corresponding the temperature of maximum weight loss ( $T_{max}$ ). The initial decomposition observed between 200–400 °C in the APP mix corresponds with the release of volatiles from the APP including  $NH_3$  and formation of crosslinked polyphosphoric acids [35]. The main decomposition process was seen from 450 to 600 °C, and  $T_{max}$  was observed at 539 °C for the APP mix. During this process, it is expected that the polyphosphoric acids may evaporate or dehydrate forming  $P_4O_{10}$  [36,37].

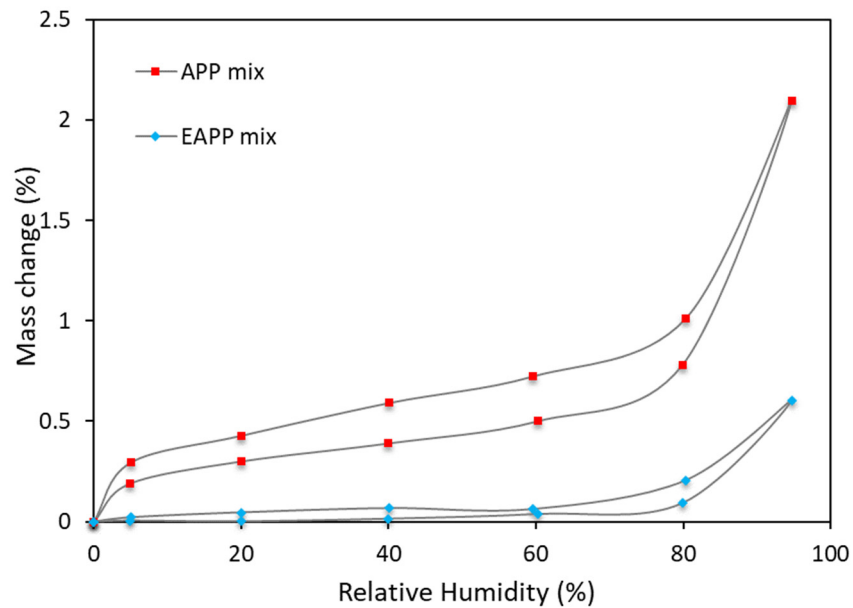


Figure 3. Vapor sorption isotherms of the intumescent blends.

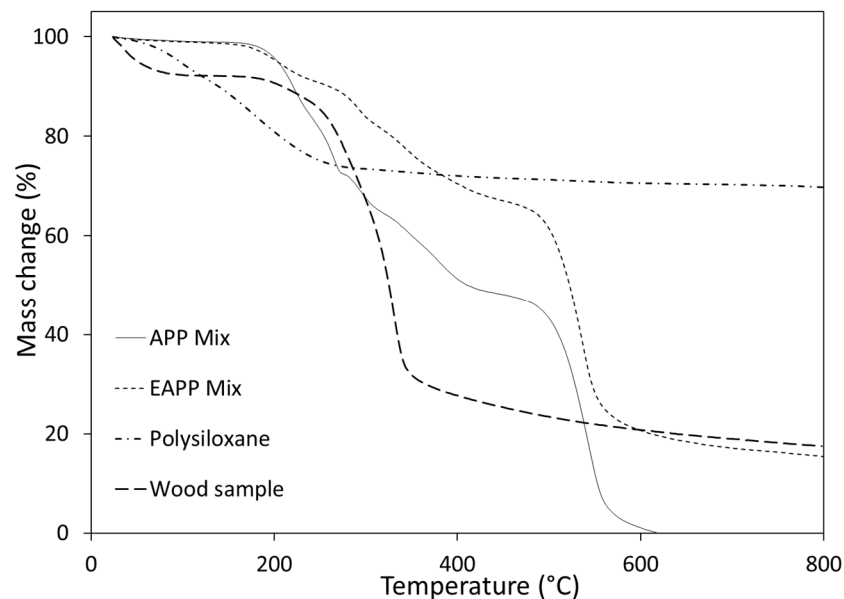


Figure 4. Thermal degradation curves of the samples.

The EAPP mix shows a similar thermal degradation behavior as the APP mix. The initial decomposition resulted in the loss of volatiles from APP. However, the initial onset temperature was slightly lesser when compared to the APP mix which could be linked with the reaction between polysiloxane and APP and faster depolymerization of APP due to the silanol [38]. The maximum weight loss of EAPP mix occurred at a similar temperature as the APP mix although the residual weight at the end was higher for the EAPP mix. Overall EAPP mix showed better thermal stability and a lower rate of mass loss when compared to the APP mix indicating that it possessed better heat resistance at higher temperatures. The reason for this could possibly be linked with the formation of silanol which reacts with the polyphosphoric acids subsequently cross-linking and forming a three-dimensional structure. It is also possible that silanol could form a compact silica shell. Both these scenarios can prevent the degradation of APP [13,39].

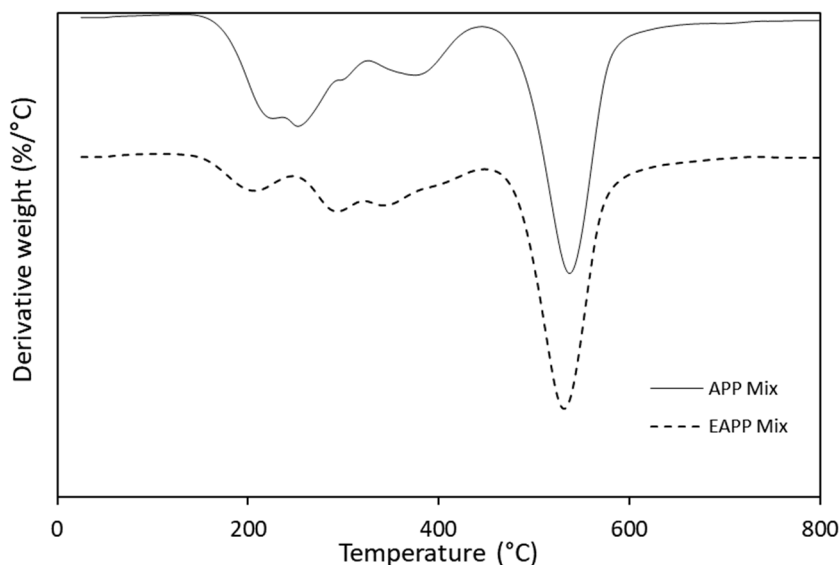


Figure 5. DTG curves of the intumescent powder blends.

The effect of polysiloxane encapsulation on flame retardant properties of the intumescent coatings was evaluated using cone calorimetry. The main parameters studied from this test were time to ignition ( $T_{\text{ign}}$ ), heat release rate (HRR), maximum peak of heat release rate ( $\text{HRR}_{\text{max}}$ ), mass loss rate (MLR), total heat release (THR) and time to maximum peak of heat release rate (Time  $\text{HRR}_{\text{max}}$ ). The cone calorimetry test was conducted on both intumescent coatings applied on wood samples (APP coating and EAPP coating) as well as control wood sample (without any coating). Another set of experiments was conducted on the intumescent coated wood samples that had undergone aging prior to the cone calorimetry test. The flame retardant properties for all samples are reported in Table 5.

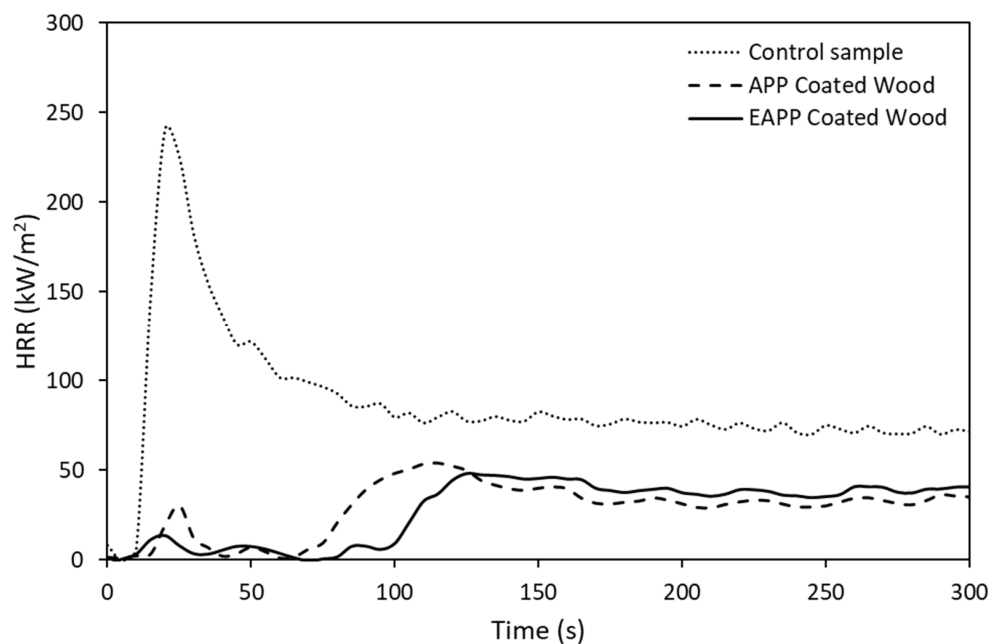
The wood samples treated with the intumescent coatings showed a delayed  $T_{\text{ign}}$  when compared to the control sample. The addition of flame retardants significantly reduced the  $\text{HRR}_{\text{max}}$  values which is the main reason for the delay in combustion. Figure 6 shows the HRR curves of the intumescent coated samples and the control sample with respect to time elapsed during the test. HRR is a measure of the heat released per unit surface area of the burning material, and it is believed to have the highest impact on fire hazard [10].

It was observed that the control wood sample burned rapidly after ignition and had a sharp  $\text{HRR}_{\text{max}}$  peak of  $240 \text{ kW/m}^2$  at about 20 s. Comparing with the control wood sample, the  $\text{HRR}_{\text{max}}$  peak of the intumescent coated wood samples decreased significantly. The  $\text{HRR}_{\text{max}}$  values of APP Coated Wood and EAPP Coated Wood were  $54$  and  $48 \text{ kW/m}^2$ , respectively, which correspondingly decreased by 77% and 80% in comparison with the control wood sample. After aging, the intumescent coated wood samples showed higher  $\text{HRR}_{\text{max}}$  values when compared to the non-aged, coated samples as reported in Table 5. However, from the HRR curves presented in Figure 7, it can be seen that the overall heat released as well as the  $\text{HRR}_{\text{max}}$  peak value was lower when compared with the control sample.

The mass loss curves of the intumescent coated wood samples and the control wood sample are presented in Figure 8 as a function of combustion time. After burning, the EAPP Coated Wood sample and the APP Coated Wood sample had residues of 28% and 22%, whereas the control wood sample had 16% residue left. As reported in Table 4, the control sample had a MLR of  $0.064 \text{ g/s}$ , and this value decreased to  $0.056$  and  $0.041 \text{ g/s}$  when the wood samples were coated with APP Coating and EAPP Coating, respectively.

**Table 5.** Fire properties of the samples from the cone calorimeter test.

Flammability Traits	Control Sample	APP Coated Wood	EAPP Coated Wood	Aged APP Coated Wood	Aged EAPP Coated Wood
Tign (s)	10 ± 2	50 ± 5	65 ± 5	10 ± 2	10 ± 2
HRR in 180 s (kW/m <sup>2</sup> )	95.64 ± 4.11	28.52 ± 1.46	26.36 ± 0.56	83.35 ± 2.91	85.77 ± 1.33
HRR in 300 s (kW/m <sup>2</sup> )	86.90 ± 3.23	30.62 ± 1.18	28.78 ± 0.81	77.46 ± 2.74	76.08 ± 0.62
HRRmax (kW/m <sup>2</sup> )	240.01 ± 9.21	54.16 ± 2.27	48.15 ± 2.73	186.19 ± 6.21	187.09 ± 3.45
MLR (g/s)	0.064 ± 0.004	0.056 ± 0.002	0.041 ± 0.001	0.057 ± 0.003	0.053 ± 0.001
THR (MJ/m <sup>2</sup> )	83.59 ± 2.19	60.59 ± 1.91	55.49 ± 0.89	74.81 ± 2.12	68.70 ± 1.56
Time HRRmax (s)	20 ± 2	115 ± 5	125 ± 5	20 ± 2	20 ± 2

**Figure 6.** HRR curves of intumescent coated wood samples and control wood sample.

After the intumescent coated wood samples were exposed to the weathering conditions, an increase in the MLR values was observed, and the residue obtained after burning was slightly higher when compared to the non-aged samples as seen in Figure 9. The THR values of all samples are also reported in Table 5. On burning, the control sample released a total heat of 83 MJ/m<sup>2</sup>, while the APP Coated Wood and EAPP Coated Wood samples released 60 and 55 MJ/m<sup>2</sup> of heat, respectively. The decrease in THR values by almost 35% for intumescent coated wood samples indicate that the modified fire retardant could significantly reduce the total heat released and enhance the fire-retardant properties of the studied samples.

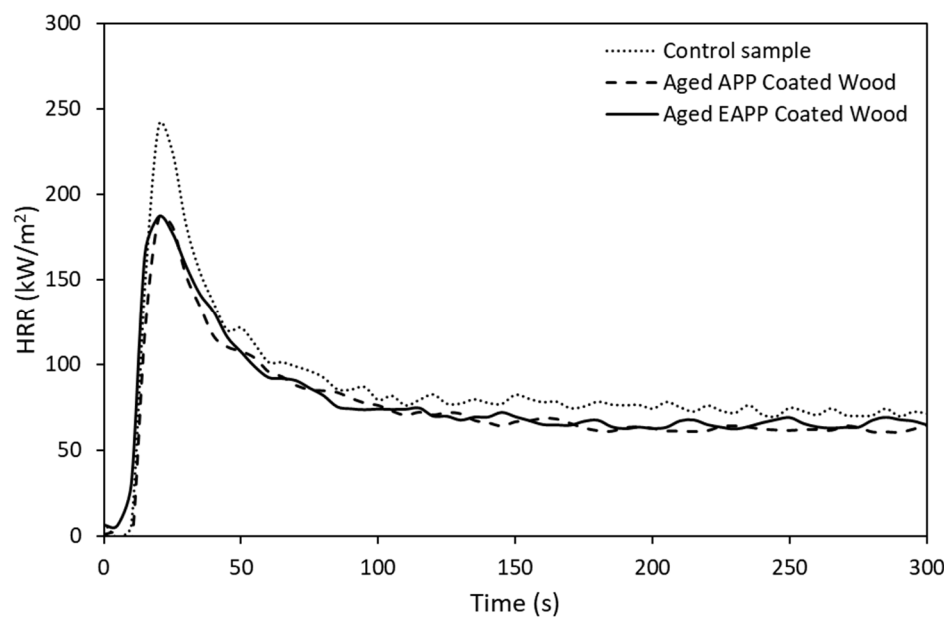


Figure 7. HRR curves of aged intumescent coated wood samples and control wood sample.

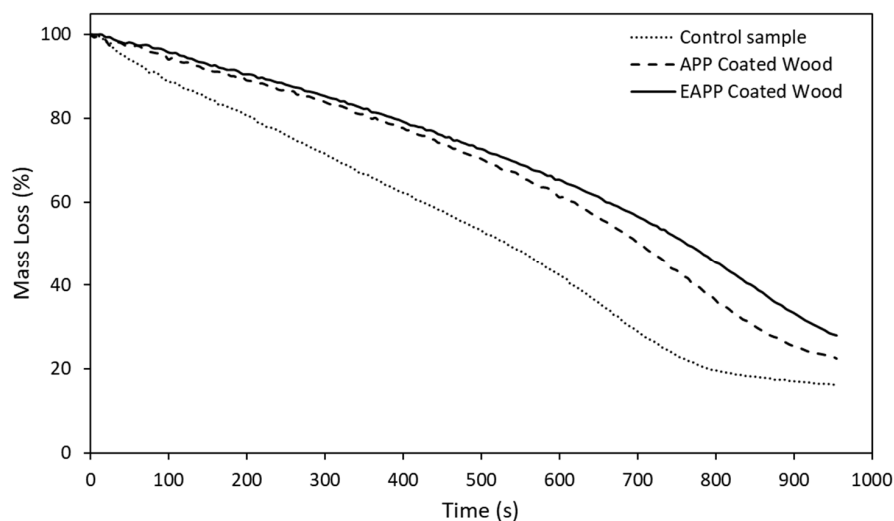
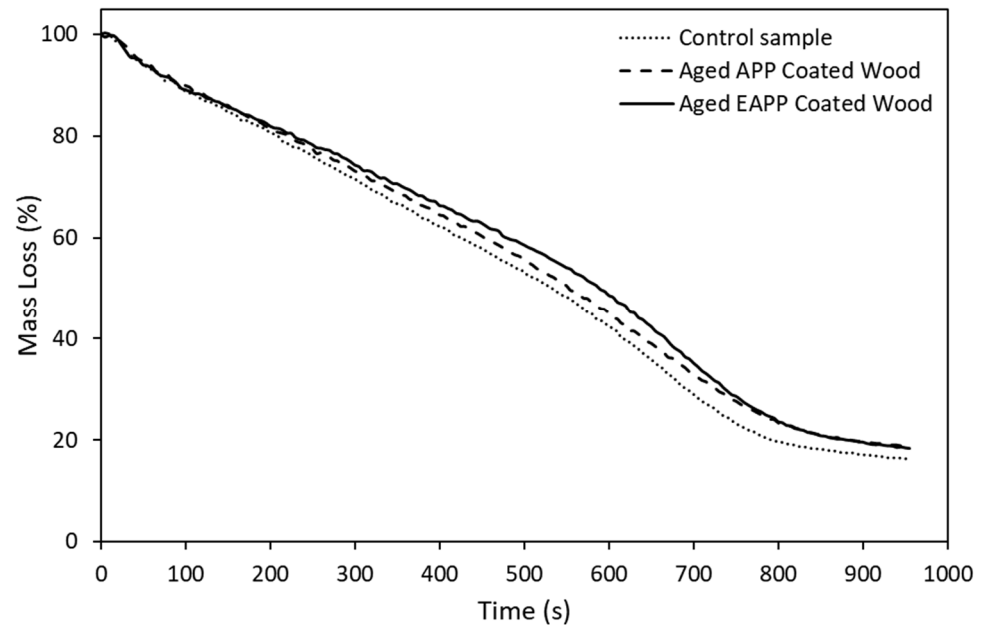


Figure 8. MLR curves of intumescent coated wood samples and control wood sample.

The organic–inorganic hybrid polysiloxane encapsulation shell has proved to enhance the water resistance of the intumescent coating. However, in extreme environmental conditions as simulated during the aging test, the microencapsulation seems to wear off leaving the fire-retardant chemicals unprotected. Both intumescent coatings have similar fire performance after undergoing aging. As seen in Table 4, the flame retardant properties ( $T_{ign}$ , HRR,  $HRR_{max}$ , THR, MLR and Time  $HRR_{max}$ ) of the intumescent coated wood samples have significantly reduced after aging, although the coatings still provide some level of fire protection to wood when compared to the non-aged control wood sample.

The FTIR spectra of polysiloxane encapsulation shell and wood samples coated with the two intumescent coatings are presented in Figure 10a. The peaks corresponding to the encapsulation shell as listed in Table 6 are seen in FTIR spectra of both, polysiloxane as well as EAPP Coated Wood sample. On the other hand, the APP coated wood sample did not show any peaks corresponding to the silica. It was observed that the coatings had a masking effect, thus lowering the peak signals of OH groups present on the wood surface.



**Figure 9.** MLR curves of aged intumescent coated wood samples and control wood sample.

The FTIR spectra of the binder and the intumescent coatings on wood after aging are presented in Figure 10b. It was observed that the binder peaks that are present in the EAPP Coated Wood and APP Coated Wood samples (Figure 10a) were not seen in the coated wood samples after aging (Figure 10b). This could possibly be interpreted as the binder being washed off or leached during the weathering experiment which also takes away most of the intumescent coating along with it [5]. This could be one of the reasons for the reduction in flame retardant properties after aging as seen in Table 5 which needs further investigation. It has been reported earlier that waterborne intumescent coatings are vulnerable to aging and also that their adhesion to substrates can be poor [15,31].

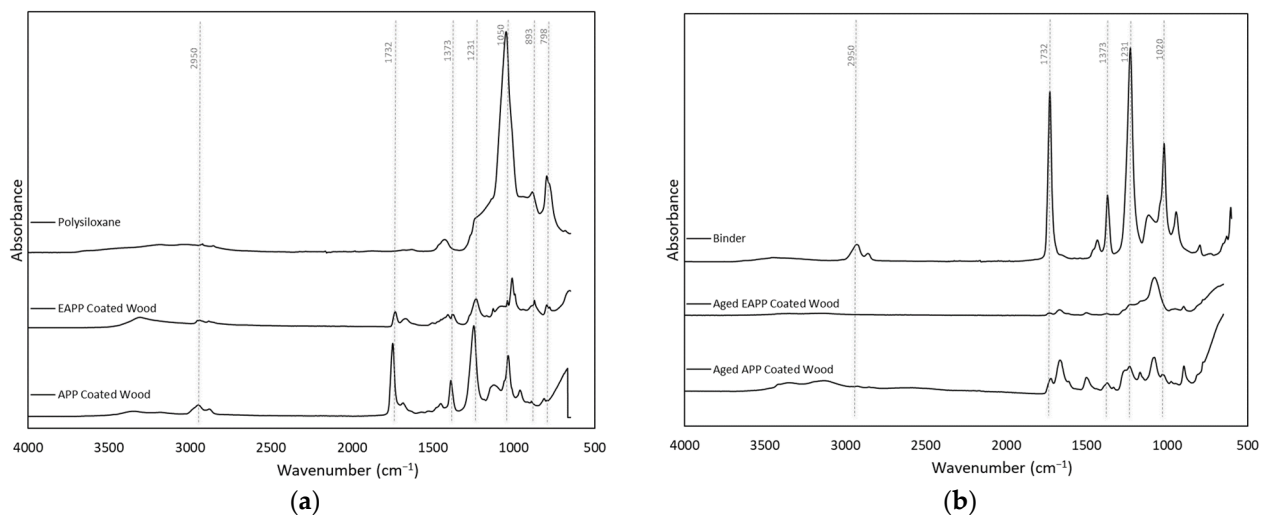


**Figure 10.** FTIR spectra for (a) polysiloxane shell and coated wood samples and (b) binder and aged coated wood samples.

**Table 6.** FTIR peaks corresponding to their respective sources.

Wavenumber (cm <sup>-1</sup> )	Vibration	Source
~3300	O–H	Polysiloxane encapsulation, wood
2930–2950	C–H vibration	Binder
1732	C=O stretch in unconjugated ketone, carbonyl and ester groups	Binder
1675	C=C stretch (weak)	Lignin in wood
1510	Aromatic skeletal vibrations C=C	Lignin in wood
1430	CH <sub>2</sub> bending	Polysiloxane encapsulation, binder
1373	CH bending	Binder
1231	C–O–C	Binder
1070	C–O stretching	Cellulose, hemicellulose in wood
1050	Si–O–Si	Polysiloxane encapsulation
1020	C–C	Binder
896	C–O–C glycosidic stretch	Polysaccharides in wood
893	Si–OH stretching	Polysiloxane encapsulation
798	Si–CH <sub>3</sub> stretching	Polysiloxane encapsulation

#### 4. Conclusions

The preparation of intumescent waterborne coatings for wood using encapsulated APP as the fire retardant is reported in this paper. The water absorption, hygroscopicity and thermal degradation of APP containing intumescent blends were significantly reduced by surface modification of APP via a polysiloxane encapsulation shell, which was prepared using the sol–gel process. The effect of the prepared intumescent coatings on the fire-retardant properties of wood was investigated using cone calorimetry. The wood samples treated with EAPP Coating possessed enhanced fire resistance showing a higher time to ignition, 80% reduction in the peak of maximum heat release, and 36% reduction in mass loss rate when compared to the control wood sample. The encapsulation of APP enhanced the physical and fire-retardant capabilities of the coating which could be attributed to the synergistic effect between APP and the polysiloxane shell. However, the coatings showed some decline in fire retardant properties after undergoing an intensive artificial accelerated weathering test, which could be due to the leaching effect as interpreted from the FTIR data. Further work is recommended on improving the durability of this coating by investigating different binder systems for enhancing its compatibility with wood. The coating penetration depth and interphase analysis can be studied to better understand the interaction between the substrate with the intumescent coating.

**Author Contributions:** Conceptualization P.B. and V.L.; methodology P.B., V.L., D.-T.H. and C.D.; formal analysis, A.H. and D.-T.H.; investigation, A.H. and D.-T.H.; resources, P.B. and V.L.; data curation, A.H. and D.-T.H.; writing—original draft preparation, A.H. and D.-T.H.; writing—review and editing, A.H., P.B. and V.L.; visualization, A.H.; supervision, P.B. and V.L.; project administration, P.B. and V.L.; funding acquisition, P.B. and V.L. All authors have read and agreed to the published version of the manuscript.

**Funding:** This research was funded by the Natural Sciences and Engineering Research Council of Canada through its IRC and CRD programs (IRCPJ 461745-18 and RDCPJ 524504-18).

**Institutional Review Board Statement:** Not applicable.

**Informed Consent Statement:** Not applicable.

**Data Availability Statement:** The data presented in this study are available on request from the corresponding author.

**Conflicts of Interest:** The authors declare no conflict of interest. The funders had no role in the design of the study; in the collection, analyses or interpretation of data; in the writing of the manuscript or in the decision to publish the results.

## References

1. Grześkowiak, W. Effectiveness of new wood fire retardants using a cone calorimeter. *J. Fire Sci.* **2017**, *35*, 565–576. [[CrossRef](#)]
2. Kaboorani, A.; Auclair, N.; Riedl, B.; Landry, V. Physical and morphological properties of UV-cured cellulose nanocrystal (CNC) based nanocomposite coatings for wood furniture. *Prog. Org. Coatings* **2016**, *93*, 17–22. [[CrossRef](#)]
3. White, R.H. Use of Coatings To Improve Fire Resistance of Wood. In *Fire Resistive Coatings: The Need for Standards*; ASTM International: West Conshohocken, PA, USA, 1983; pp. 24–39. [[CrossRef](#)]
4. Lowden, L.; Hull, T. Flammability behaviour of wood and a review of the methods for its reduction. *Fire Sci. Rev.* **2013**, *2*, 4. [[CrossRef](#)]
5. Goldsmith, F.P. *Fire Retardant Coatings: An Evaluation of Fire Retardant Coatings as a Means of Protecting Wood Panels*; University of British Columbia Library: Vancouver, BC, Canada, 2011.
6. Mariappan, T. Recent developments of intumescent fire protection coatings for structural steel: A review. *J. Fire Sci.* **2016**, *34*, 120–163. [[CrossRef](#)]
7. Sun, F.C.; Fu, J.H.; Peng, Y.X.; Jiao, X.M.; Liu, H.; Du, F.P.; Zhang, Y.F. Dual-functional intumescent fire-retardant/self-healing water-based plywood coatings. *Prog. Org. Coatings* **2021**, *154*, 106187. [[CrossRef](#)]
8. Aziz, H.; Ahmad, F. Effects from nano-titanium oxide on the thermal resistance of an intumescent fire retardant coating for structural applications. *Prog. Org. Coatings* **2016**, *101*, 431–439. [[CrossRef](#)]
9. Eremina, T.; Korolchenko, D. Fire protection of building constructions with the use of fire-retardant intumescent compositions. *Buildings* **2020**, *10*, 185. [[CrossRef](#)]
10. Liu, Y.; Deng, C.L.; Zhao, J.; Wang, J.S.; Chen, L.; Wang, Y.Z. An efficiently halogen-free flame-retardant long-glass-fiber-reinforced polypropylene system. *Polym. Degrad. Stab.* **2011**, *96*, 363–370. [[CrossRef](#)]
11. Alongi, J.; Han, Z.; Bourbigot, S. Intumescence: Tradition versus novelty. A comprehensive review. *Prog. Polym. Sci.* **2014**, *51*, 28–73. [[CrossRef](#)]
12. Bellayer, S.; Jimenez, M.; Barrau, S.; Bourbigot, S. Fire retardant sol-gel coatings for flexible polyurethane foams. *RSC Adv.* **2016**, *6*, 28543–28554. [[CrossRef](#)]
13. Deng, C.L.; Du, S.L.; Zhao, J.; Shen, Z.Q.; Deng, C.; Wang, Y.Z. An intumescent flame retardant polypropylene system with simultaneously improved flame retardancy and water resistance. *Polym. Degrad. Stab.* **2014**, *108*, 97–107. [[CrossRef](#)]
14. Kumar, M.; Kumar, M.; Arora, S. Thermal degradation and flammability studies of wood coated with fly ash intumescent composites. *J. Indian Acad. Wood Sci.* **2013**, *10*, 125–133. [[CrossRef](#)]
15. Popescu, C.M.; Pfriem, A. Treatments and modification to improve the reaction to fire of wood and wood based products—An overview. *Fire Mater.* **2020**, *44*, 100–111. [[CrossRef](#)]
16. Wang, B.; Sheng, H.; Shi, Y.; Hu, W.; Hong, N.; Zeng, W.; Ge, H.; Yu, X.; Song, L.; Hu, Y. Recent advances for microencapsulation of flame retardant. *Polym. Degrad. Stab.* **2015**, *113*, 96–109. [[CrossRef](#)]
17. Idumah, C.I. Emerging advancements in flame retardancy of polypropylene nanocomposites. *J. Thermoplast. Compos. Mater.* **2020**. [[CrossRef](#)]
18. Kazanci, B.; Cellat, K.; Paksoy, H. Preparation, characterization, and thermal properties of novel fire-resistant microencapsulated phase change materials based on paraffin and a polystyrene shell. *RSC Adv.* **2020**, *10*, 24134–24144. [[CrossRef](#)]
19. Huang, Z.; Ruan, B.; Wu, J.; Ma, N.; Jiang, T.; Tsai, F.C. High-efficiency ammonium polyphosphate intumescent encapsulated polypropylene flame retardant. *J. Appl. Polym. Sci.* **2021**, *138*, 50413. [[CrossRef](#)]
20. Lazar, S.T.; Kolibaba, T.J.; Grunlan, J.C. Flame-retardant surface treatments. *Nat. Rev. Mater.* **2020**, *5*, 259–275. [[CrossRef](#)]
21. Wang, B.; Wang, X.; Tang, G.; Shi, Y.; Hu, W.; Lu, H.; Song, L.; Hu, Y. Preparation of silane precursor microencapsulated intumescent flame retardant and its enhancement on the properties of ethylene–vinyl acetate copolymer cable. *Compos. Sci. Technol.* **2012**, *72*, 1042–1048. [[CrossRef](#)]
22. Qiu, J.; Lai, X.; Li, H.; Gao, J.; Zeng, X.; Liao, X. Facile fabrication of a novel polyborosiloxane-decorated layered double hydroxide for remarkably reducing fire hazard of silicone rubber. *Compos. Part B Eng.* **2019**, *175*, 107068. [[CrossRef](#)]
23. Xu, B.; Wu, X.; Ma, W.; Qian, L.; Xin, F.; Qiu, Y. Synthesis and characterization of a novel organic-inorganic hybrid char-forming agent and its flame-retardant application in polypropylene composites. *J. Anal. Appl. Pyrolysis* **2018**, *134*, 231–242. [[CrossRef](#)]
24. Wilke, A.; Langfeld, K.; Ulmer, B.; Andrievici, V.; Hörold, A.; Limbach, P.; Bastian, M.; Scharrel, B. Halogen-free multicomponent flame retardant thermoplastic styrene–ethylene–butylene–styrene elastomers based on ammonium polyphosphate–expandable graphite synergy. *Ind. Eng. Chem. Res.* **2017**, *56*, 8251–8263. [[CrossRef](#)]
25. Ran, G.; Liu, X.; Guo, J.; Sun, J.; Li, H.; Gu, X.; Zhang, S. Improving the flame retardancy and water resistance of polylactic acid by introducing polyborosiloxane microencapsulated ammonium polyphosphate. *Compos. Part B Eng.* **2019**, *173*, 106772. [[CrossRef](#)]
26. Liu, X.; Sun, J.; Zhang, S.; Guo, J.; Tang, W.; Li, H.; Gu, X. Effects of carboxymethyl chitosan microencapsulated melamine polyphosphate on the flame retardancy and water resistance of thermoplastic polyurethane. *Polym. Degrad. Stab.* **2019**, *160*, 168–176. [[CrossRef](#)]
27. Jia, Y.-W.; Zhao, X.; Fu, T.; Li, D.-F.; Guo, Y.; Wang, X.-L.; Wang, Y.-Z. Synergy effect between quaternary phosphonium ionic liquid and ammonium polyphosphate toward flame retardant PLA with improved toughness. *Compos. Part B Eng.* **2020**, *197*, 108192. [[CrossRef](#)]
28. Hoang, D.T.; Schorr, D.; Landry, V.; Blanchet, P.; Vanslambrouck, S.; Dagenais, C. Preparation and characterisation of flame retardant encapsulated with functionalised silica-based shell. *J. Microencapsul.* **2018**, *35*, 428–438. [[CrossRef](#)] [[PubMed](#)]

29. Wang, S.; Jiang, Y.; Meng, Y.; Li, Y.; Han, Z.; Liu, X.; Li, H.; Sun, J.; Fei, B.; Gu, X.; et al. The encapsulation of intumescent flame retardants by poly-siloxane for thermoplastic polyolefin: Fire safety and water resistance. *Polym. Degrad. Stab.* **2021**, *188*, 109561. [[CrossRef](#)]
30. Li, R.-M.; Deng, C.; Deng, C.-L.; Dong, L.-P.; Di, H.-W.; Wang, Y.-Z. An efficient method to improve simultaneously the water resistance, flame retardancy and mechanical properties of POE intumescent flame-retardant systems. *RSC Adv.* **2015**, *5*, 16328–16339. [[CrossRef](#)]
31. Liu, Z.; Dai, M.; Zhang, Y.; Gao, X.; Zhang, Q. Preparation and performances of novel waterborne intumescent fire retardant coatings. *Prog. Org. Coatings* **2016**, *95*, 100–106. [[CrossRef](#)]
32. Shen, M.Y.; Chen, W.J.; Kuan, C.F.; Kuan, H.C.; Yang, J.M.; Chiang, C.L. Preparation, characterization of microencapsulated ammonium polyphosphate and its flame retardancy in polyurethane composites. *Mater. Chem. Phys.* **2016**, *173*, 205–212. [[CrossRef](#)]
33. Hussain, A.; Calabria-Holley, J.; Jiang, Y.; Lawrence, M. Modification of hemp shiv properties using water-repellent sol-gel coatings. *J. Sol-Gel Sci. Technol.* **2018**, *86*, 187–197. [[CrossRef](#)]
34. Hussain, A.; Calabria-Holley, J.; Lawrence, M.; Jiang, Y. Resilient hemp shiv aggregates with engineered hygroscopic properties for the building industry. *Constr. Build. Mater.* **2019**, *212*, 247–253. [[CrossRef](#)]
35. Camino, G.; Grassie, N.; McNeill, I.C. Influence of the fire retardant, ammonium polyphosphate, on the thermal degradation of poly(methyl methacrylate). *J. Polym. Sci. Polym. Chem. Ed.* **1978**, *16*, 95–106. [[CrossRef](#)]
36. Ni, J.; Chen, L.; Zhao, K.; Hu, Y.; Song, L. Preparation of gel-silica/ammonium polyphosphate core-shell flame retardant and properties of polyurethane composites. *Polym. Adv. Technol.* **2011**, *22*, 1824–1831. [[CrossRef](#)]
37. Wu, K.; Wang, Z.; Hu, Y. Microencapsulated ammonium polyphosphate with urea-melamine-formaldehyde shell: Preparation, characterization, and its flame retardance in polypropylene. *Polym. Adv. Technol.* **2008**, *19*, 1118–1125. [[CrossRef](#)]
38. Gao, S.; Li, B.; Bai, P.; Zhang, S. Effect of polysiloxane and silane-modified SiO<sub>2</sub> on a novel intumescent flame retardant polypropylene system. *Polym. Adv. Technol.* **2011**, *22*, 2609–2616. [[CrossRef](#)]
39. Lin, H.; Yan, H.; Liu, B.; Wei, L.; Xu, B. The influence of KH-550 on properties of ammonium polyphosphate and polypropylene flame retardant composites. *Polym. Degrad. Stab.* **2011**, *96*, 1382–1388. [[CrossRef](#)]